Clays and Clay Minerals, Vol. 61, No. 3, 165–176, 2013.

FEASIBLE SYNTHESIS OF TiO_2 DEPOSITED ON KAOLIN FOR PHOTOCATALYTIC APPLICATIONS

JIŘÍ HENYCH* AND VÁCLAV ŠTENGL

[1] Department of Solid State Chemistry, Institute of Inorganic Chemistry AS CR v.v.i., 250 68 Husinec-Řež, Czech Republic
[2] Faculty of the Environment, University of Jan Evangelista Purkyně, Králova Výšina 7, 400 96 Ústí nad Labem, Czech Republic

Abstract— The aim of the present study was to synthesize a photocatalyst on the basis of TiO_2 with kaolin as the support material. Properties such as layered structure and a suitable particle size of kaolin could be beneficial in the production of a high-quality and relatively cheap photocatalyst on an industrial scale. Homogeneous hydrolysis with urea as a precipitation agent and kaolin as support material was used to obtain a kaolin surface covered with TiO_2. Samples were characterized by means of X-ray powder diffraction, infrared and Raman spectroscopy, high-resolution transmission electron microscopy, Brunauer-Emmett-Teller surface area, and Barrett-Joyner-Halenda porosity determination. Photocatalytic activity was assessed by a Reactive Black 5 azo dye discoloration in a water suspension and by acetone decomposition on a thin layer of sample in a gas phase. The characterization confirmed that the well crystallized TiO_2 was distributed effectively over the whole surface of a kaolin substrate, and photocatalytic tests revealed that the active surface layer of titania particles on kaolin performed well, suggesting that kaolin acts as a suitable support.

Key Words—Homogeneous Hydrolysis, Kaolin, Photocatalysis, TiO_2, Urea.

INTRODUCTION

Among photocatalysts, titanium dioxide is one of the most popular and widely used in spite of known drawbacks such as low performance under Vis light and agglomeration of the nanoparticles. Its stability, non-toxicity, and relatively small preparation costs can meet growing demands for sustainable, green technologies. A sol-gel route based on the controlled hydrolysis of an alkoxide (Gupta and Tripathi, 2012; Trentler *et al.*, 1999; Wang and Ying, 1999) is one of the methods of synthesis used most often. This is because structure modifications such as doping (Hamal and Klabunde, 2007) or the growth of tailored structures (Choi *et al.*, 2006) are relatively easy to achieve. Aside from alkoxides, the commonly used starting materials are titanium(IV) chloride and titanium(IV) sulfate. For preparation on an industrial scale, organometallic compounds in non-water solvents or high reactivity can be used; exothermal reaction with water and acids of $TiCl_4$ are problematic. Because of these problems, a method of homogeneous hydrolysis of $TiOSO_4$ in the presence of urea (Stengl *et al.*, 2003b) could be used as it provides highly active, well defined anatase crystals suitable for use in photocatalytic applications.

Recent literature has reported a number of attempts at the preparation of composite materials, where the main focus has been to use a highly functional surface layer with proper support, or a composite medium, which can produce the desired effects: change the properties of the materials, reduce the cost of production sufficiently, or even allow application at industrial scale. Titania-pillared clays have been researched extensively (Ding *et al.*, 2008; Mao *et al.*, 2010; Yamanaka *et al.*, 1987). They have a mesoporous structure due to the small TiO_2 particles which are located as pillars between the silicate layers and show significant adsorption ability due to the large specific surface area (Choy *et al.*, 1998; Ding *et al.*, 2001; Hermosin *et al.*, 1993). The combination of the TiO_2 with clay minerals for a photocatalytic purpose has also become an attractive sector of current research. Because the structure properties are crucial for photocatalysis, the effects of clay minerals in composites on the structure have been evaluated (Belessi *et al.*, 2007; Kun *et al.*, 2006) to effectively control the properties. Yang *et al.* (2008) assessed the effect of a desired mesoporous structure of the beidellite clay/TiO_2 composite synthesized under a hydrothermal treatment for phenol photodegradation under UV light. Investigations by Ahn *et al.* (2009) and Jiang *et al*. (2013) showed that the photocatalytic activity could be improved by forming a mesoporous system. Adsorption is another significant phenomenon influencing the activity of titania, and fine-tuning the ability of the new material to adsorb pollutants is the aim of many research groups. Montmorillonite modified with hexadecylpyridinium chloride (HDPM) in TiO_2 suspensions for 2-chlorophenol (2-CP) degradation was used as an adsorption agent (Mogyorosi *et al.*, 2002). Better degradation was observed (Menesi *et al.*, 2008) on TiO_2/Ca-montmorillonite composites prepared by wet grinding in an

* E-mail address of corresponding author:
henych@iic.cas.cz
DOI: 10.1346/CCMN.2013.0610301

agate mill than on pure TiO_2. Vanadium-doped TiO_2-montmorillonite nanocomposites were prepared by Chen *et al.* (2011b) using a simple sol-gel method for the photodegradation of sulforhodamine B under visible light irradiation, where the layer silicate of montmorillonite behaves as a barrier that prevents TiO_2 powders from agglomerating. Composites also have a larger surface area and V doping can improve the photoabsorption. Titania-impregnated kaolinite was synthesized (Chong *et al.*, 2009) in an attempt to solve the problem of separating the photocatalyst from the water after treatment. A TiO_2/clay composite can be separated readily unlike very small particles of pure TiO_2. This composite, prepared by a two-step sol-gel process, was effective for Congo red decomposition in a water suspension. A study of the evaluation of the physical properties and photodegradation capacity was carried out on titania impregnated into modified kaolin by the sol-gel process (Vimonses *et al.*, 2010) where TiO_2 nanocrystallites were deposited uniformly on the kaolin external surface, resulting in a high degree of photon activation. An interesting comparative study of adsorption and degradation on several volatile organic compound sample pollutants by a combined titania-montmorillonite-silica photocatalyst was carried out by Chen *et al.* (2011a). The present study demonstrates the possibility of using alternative cheaper materials which, because of their structure, are more suitable as supports; proper analysis has not been done, however.

The main aim of the present study was to synthesize a highly active photocatalyst based on titania particles using a kaolinite as a support material, which can effectively prevent agglomeration of the small TiO_2 particles, affect the sorption capacity, and, thanks to the price of kaolin, reduce the cost of production. To test whether titania nanocrystals would: preserve their crystallinity without impurities, maintain good photocatalytic performance, and be distributed over all of the kaolinite surface, several materials-characterization methods were used. Finally, because of the growing demands for 'green technologies,' another condition was to use an environmentally benign method for industrial production. A straightforward, cheap, 'one-pot' method for preparing highly active titania nanocrystals, based on the homogeneous hydrolysis of an aqueous solution of $TiOSO_4$ in a suspension of kaolin, is demonstrated here. Titania was deposited effectively on the surface of kaolin, which serves as a support material. The samples with varying amounts of titania were characterized and tested for photocatalytic discoloration of RB5 azo dye in water slurries and for acetone degradation in a gas phase.

EXPERIMENTAL

Synthesis of samples

Chemicals used were titanium oxo-sulfate, $TiOSO_4$; urea, $(NH_2)_2CO$; and H_2SO_4, which were of analytical grade and supplied by Fluka and Sigma-Aldrich Ltd, Germany. The substrate for reaction, kaolin, which was purchased from the Czech industrial producer České lupkové závody, a.s. (ČLUZ), originated from the acclaimed Czech deposits in Eger Graben in the western part of the Czech Republic, used for many decades in the production of ceramics. This kaolin, denoted as KDG, consists almost entirely of kaolinite (see below), with about equal proportions of the particle size fractions of 0.1−2 μm (55%) and 2−20 μm (45%).

The surface layers of TiO_2 nanocrystals were prepared by the hydrolysis of sulfate aqueous solutions using urea as a precipitation agent. The homogeneous precipitation or hydrolysis differs significantly from the more common, simple technique of adding neutralization agents (Li *et al.*, 2010). Solutions prepared by homogenous precipitation contain the precipitating agents (OH^-, SH^-, or H_2S) produced by a chemical reaction in the bulk of the solution without local supersaturation. For instance, urea and thioacetamide can be used as the precipitating agents instead of ammonia and hydrogen sulfide, respectively. A temperature of >60ºC leads to a decomposition of urea to produce OH^- ions:

$$(NH_2)_2CO + 2\ H_2O \rightarrow CO_2\uparrow + NH_4OH + NH_3 \quad (1)$$
$$NH_3 + H_2O \rightarrow NH_4^+ + OH^- \quad (2)$$
$$Me^{2+} + 2\ OH^- \rightarrow Me(OH)_2 \quad (3)$$
$$Ti^{4+} + 4\ OH- \rightarrow Ti(OH)_4 \quad (4)$$

A gradual evolution of ammonium (1) causes a pH increase (2), which leads to the gradual precipitation of hydroxides or oxides of the dissolved metal cations present (3); reaction 4 refers to the case of Ti^{4+}. The products of these reactions are mostly spherical agglomerates with a well developed microstructure and a large surface area (>300 m^2g^{-1}) which can easily be filtered out.

Various amounts of $TiOSO_4$ (see Table 1) were diluted in 500 mL of hot water (70ºC) acidified by 98% H_2SO_4 to pH ~2−3. 100 g of kaolin was added to the pellucid liquid, and the mixture was diluted with

Table 1. Surface area and pore volume of kaolin and prepared TiO_2 and kaolin/TiO_2 from variable amounts of $TiOSO_4$.

Sample	$TiOSO_4$ (g)	$TiOSO_4$ conc. (M)	BET (m^2g^{-1})	Total pore volume (cm^3g^{-1})
KDG	–	–	12	0.065
pure TiO_2	100	1.25	291	0.240
TiKDG25	25	0.31	46	0.084
TiKDG50	50	0.63	64	0.125
TiKDG75	75	0.94	83	0.166
TiKDG100	100	1.25	86	0.199
TiKDG125	125	1.56	92	0.188

https://doi.org/10.1346/CCMN.2013.0610301 Published online by Cambridge University Press

distilled water to a total volume of 4 L. To the solution was added 300 g of urea and the mixture was heated at 95–100ºC under stirring for 6 h until pH 7.2–7.5 was reached and ammonia escaped from the solution. The precipitates formed were washed with distilled water, filtered out (using 5 μm filter paper), and the solids were air dried at ambient temperature.

For the photocatalytic tests in a gas phase, the titania/kaolin powder prepared (2 g) was dispersed in a mixture of 5 mL of poly(hydroxyethyl methacrylate) and 10 mL of ethanol. From this suspension, a layer 300 μm thick (~1 g) was deposited on a 100 mm × 150 mm glass plate.

CHARACTERIZATION METHODS

Diffraction patterns were collected with a PANalytical XPert PRO diffractometer equipped with a conventional X-ray tube (CuKα radiation, 40 kV, 30 mA) and a PIXcel linear position-sensitive detector with an antiscatter shield. A programmable divergence slit set to a fixed value of 0.5, Soller slits of 0.02 rad, and a mask (an integral part of the Xpert Pro diffractometer used to define the size of the primary beam on the sample in the perpendicular direction). A programmable antiscatter slit set to a fixed value of 0.5, a Soller slit of 0.02 rad, and a Ni β filter were used in the diffracted beam. Phase identification was performed using the *DiffracPlus Eva* software package (Bruker AXS GmbH, Karlsruhe, Germany) using the JCPDS PDF-2 database (2001).

Transmission electron micrographs were obtained using a JEOL JEM 3010 microscope operated at 300 kV (LaB_6 cathode). A copper-grid coated with a holey carbon support film was used to prepare samples for HRTEM observation. The powdered sample was dispersed in ethanol and the suspension treated in an ultrasonic bath for 10 min.

The specific surface areas of samples were determined from the nitrogen adsorption-desorption isotherms at liquid nitrogen temperature using a Coulter SA3100 instrument with 15 min of outgas at 150ºC. The Brunauer-Emmett-Teller (BET) method (Brunauer *et al.*, 1938) was used for the surface-area calculation and the pore-size distribution (pore diameters, pore volumes, and micropore surface areas of the samples) was determined using the Barrett-Joyner-Halenda (BJH) method (Barrett *et al.*, 1951).

Raman spectra were obtained using a DXR Raman microscope (Thermo Fisher Scientific, Waltham, Massachussets, USA). A 532 nm laser was used at a power of 3 mW. Powdered samples were scanned using a 15 point mapping mode under a 10× objective lens with an automated autofocus at each point to get 15 random measurements.

The photocatalytic activity in solution was assessed from the kinetics of the photocatalytic degradation of RB5 dye in aqueous slurries. The kinetic curves obtained were processed by fitting exponential models using the *Origin* software (OriginLab, Northampton, USA) as described by Stengl *et al*. (2009). In contrast to methylene blue, the azo dyes (Orange II, Methyl Red, RB5, Congo Red, *etc*.) are not adsorbed on titania surfaces and, hence, their photodecomposition is evaluated simply from the concentration of the remaining dissolved dye. Degradation of azo groups –N=N– in azo dyes leads to N_2 (Lachheb *et al.*, 2002 and Guillard *et al.*, 2003), which is ideal for the elimination of pollutants containing nitrogen for environmental photocatalysis or any other physico-chemical method.

The kinetics of photocatalytic degradation of an aqueous RB5 dye solution was measured by using a homemade photoreactor (Stengl *et al.*, 2008a), which consisted of a stainless steel cover and a quartz tube with a Narva fluorescent lamp (UV, Black-light 365 nm) having a power of 13 W and a light intensity of ~3.5 mW cm^{-2}. One liter of a 0.5 mM RB5 dye solution was circulated by means of a membrane pump using a flow-through measuring cell. Before the lamp was switched on, the suspension was mixed in the dark for 30 min to establish the adsorption-desorption equilibrium. The concentration of RB5 dye was determined by measuring the absorbance at 590 nm with a ColorQuestXE visible-light spectrophotometer. A 0.5 g portion of sample was sonicated for 10 min in an ultrasonic bath (300 W and 35 kHz) before the kinetic tests. The pH of the resulting suspension was taken as the initial value for neutral conditions. In the gas phase, the kinetics of the photocatalytic degradation of acetone was examined using a homemade stainless-steel batch photoreactor (which has a different shape, volume, valves, dosing, and detection system) (Ctibor *et al.*, 2011) with a Narva black-light fluorescent lamp at wavelength 365 nm (input power 8 W, light intensity 6.3 mW cm^{-2}). The gas concentration was measured by a quadrupole mass spectrometer JEOL JMS-Q100GC and gas chromatograph Agilent 6890N. A high-resolution gas chromatography column (19091P-QO4, J&W Scientific) was used. Samples were taken from the reactor in a time interval of 2 h automatically through the sampling valve (six-port external volume sample injector from Valco Instruments Co., Inc, Vici AG International, Schenkon, Switzerland).

Blank tests (a layer of poly(hydroxyethyl methacrylate) without titania) were performed to establish the effect of photolysis and catalysis on the conversion of acetone. The UV irradiation detected no measurable conversion of acetone, as a testing substance, into CO and/or CO_2, and no acetone was adsorbed on the poly(hydroxyethyl methacrylate) matrix. The injection volume of acetone into the photoreactor was 2 mL. The total volume of the reactor was 3.5 L, filled with oxygen, at a flow rate of 1 L/min.

https://doi.org/10.1346/CCMN.2013.0610301 Published online by Cambridge University Press

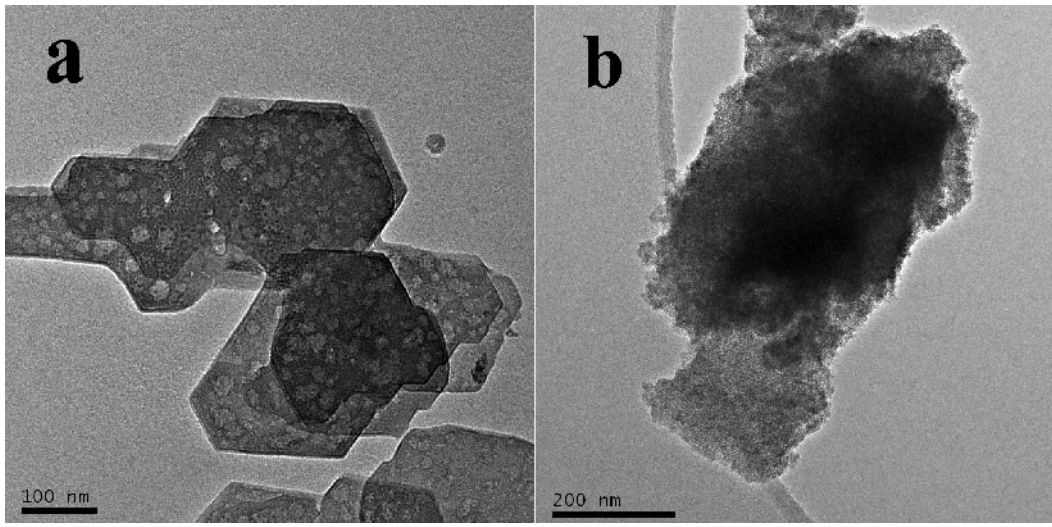

Figure 1. HRTEM images: (a) bare kaolin substrate; (b) kaolin surface covered by TiO_2 nanocrystals.

RESULTS AND DISCUSSION

If the proper composition of the parent solution was found empirically and the correct heating rate was chosen in the presence of a suitable substrate (*i.e*. mica (Stengl *et al.*, 2003a), kaolin, or cellulose) in the reaction mixture, the resulting hydrolysis products have a tendency to cover that substrate with a thin surface layer. In this case, the bare kaolin substrate (Figure 1a) after reaction was coated with small titania particles (Figure 1b). Note that the surface of the kaolin particles depicted was covered by TiO_2 crystals. The uniformity of the distribution of the particles is a desired effect, consequently providing a large specific surface area for photocatalytic reaction. Kaolin was, therefore, shown to be a good supporting material.

The results from XRD analysis of the TiO_2/kaolin composites synthesized (Figure 2) showed the sharp diffraction lines typical of kaolinite (PDF 89-6538) in all samples. A precipitated anatase fraction (PDF 21-1272) was also noted, though the peaks were somewhat less distinct due to the smaller amount and significantly smaller titania particles compared to those of kaolinite. No crystalline phase impurities were observed. Rietveld refinement could not be employed because of the overlapping of the peaks of well crystallized kaolinite and broad, weak peaks of titania. Nevertheless, the size of the coherent domain of the titania particles prepared by homogeneous hydrolysis was a few tens or several nm, as described previously (Stengl *et al*., 2003b, 2008b).

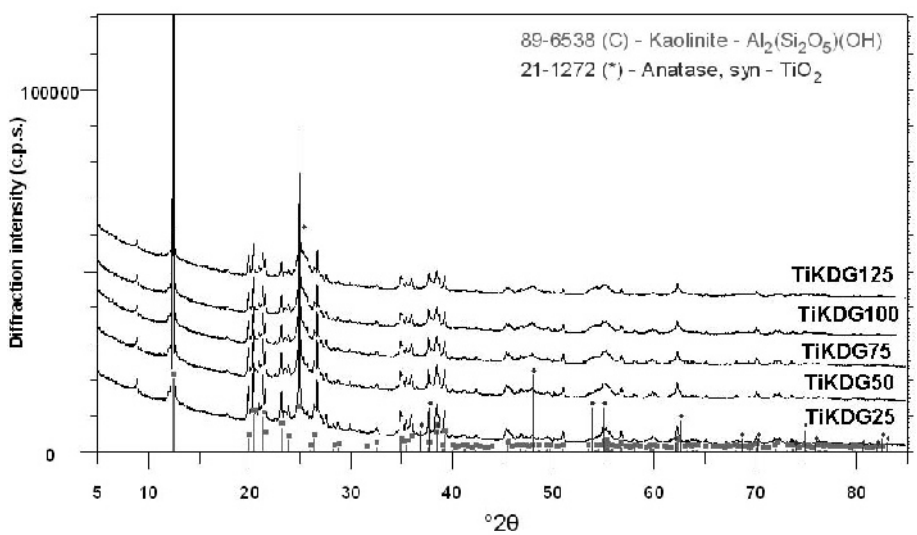

Figure 2. XRD patterns of synthesized TiO_2/kaolin samples.

https://doi.org/10.1346/CCMN.2013.0610301 Published online by Cambridge University Press

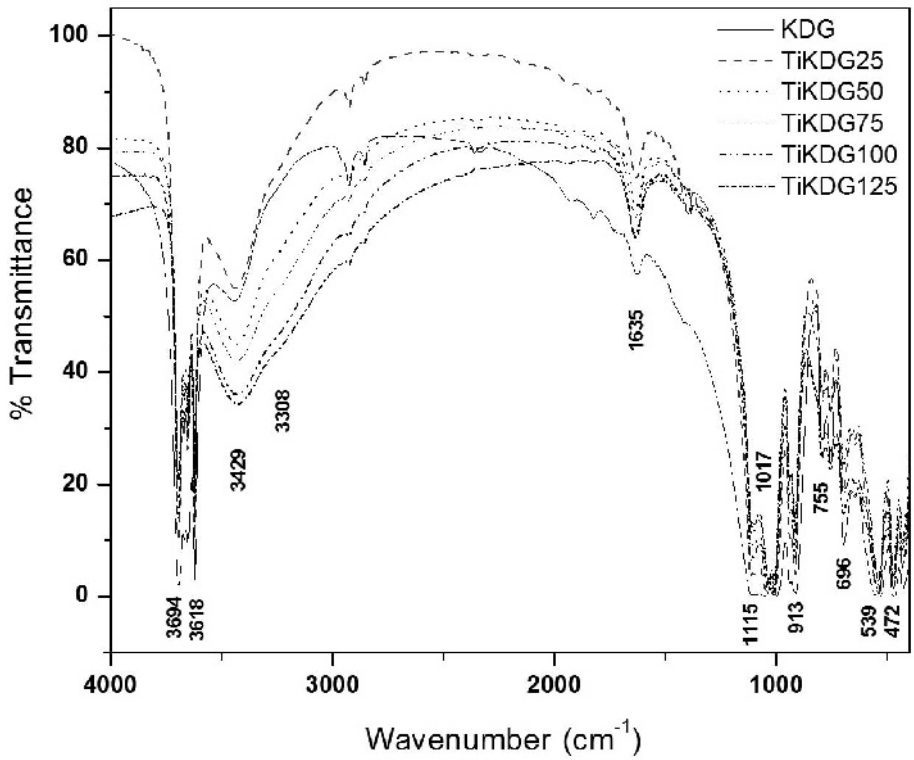

Figure 3. FTIR spectra of kaolin samples coated with TiO_2.

Four characteristic bands for kaolinite in the OH-stretching region at 3694, 3669, 3645, and 3618 cm^{-1} were distinguished in the infrared (IR) spectra of kaolin samples coated with TiO_2 (Figure 3) (Robin *et al.*, 2013). Only four OH groups are present in the kaolinite unit cell (Bish, 1993), but because of their dichroic behavior the one-to-one assignment of these bands to the respective individual OH groups is risky (Farmer, 1974; Johnston *et al.*, 1990). The bands observed at positions around 1115 cm^{-1} and 1017 cm^{-1} were attributed to Si−O stretching vibrations. The Al-OH deformation band was observed at 913 cm^{-1}. The band positions at ~755 cm^{-1}, 696 cm^{-1}, and 539 cm^{-1} are part of the Si−O−Al vibrations (Kutlakova *et al.*, 2011; Saikia and Parthasarathy, 2010). Infrared spectroscopy revealed no remnants of anions from the synthesis.

Raman spectroscopy is an established technique for studying crystal structures. Kaolin has only a weak Raman spectrum, whereas anatase has significant specific vibration modes located around 150 cm^{-1} (Eg), 399 cm^{-1} (B1g), 515 cm^{-1} (B1g+A1g), and 638 cm^{-1} (Eg) (Ohsaka *et al.*, 1978). In the spectrum (Figure 4) of kaolin by itself (sample KDG), a peak at 143 cm^{-1} was seen, representing a small admixture of anatase; Raman spectroscopy allows detection of concentrations down to 0.02% of anatase in the kaolin structure (Murad, 1997). With increasing amount of Ti precursor added, the typical vibration modes of anatase became more intense, suggesting well formed crystalline particles of TiO_2 in the samples synthesized. The shift in position and the broadening of the Raman band relative to well crystallized anatase were consistent with the nanocrystalline nature and presence of defects in the anatase structure (Stengl and Matys Grygar, 2011).

The multipoint BET method for the specific surface area and BJH method for pore size and volume determination was employed (Table 1). No micropores were found in any of the samples. Titania prepared by homogeneous hydrolysis (Stengl and Matys Grygar, 2011) possesses the typical type IV isotherm with H2 hysteresis loop, according to IUPAC notation (Sing *et al.*, 1985) which characterizes materials with a good mesoporous structure. The samples of kaolin with titania (Figure 5 inset) had a type II isotherm, suggesting that supporting kaolin had either no pores or only macropores (>50 nm). The H3 hysteresis loop corresponds to aggregates of plate-like particles giving rise to slit-like pores and to solids with very wide pore-size distribution (Chang *et al.*, 2009), which could be expected of a kaolinite surface covered with mesoporous titania. All TiKDG samples had wide pore-size distributions (Figure 6) and an increasing proportion of TiO_2 led to the large volume of N_2 adsorbed, thanks to the large surface area of pure titania crystals. This effect was also seen from the adsorption-desorption isotherms (Figure 7) where, with a larger amount of titania, the isotherm clearly became steeper and closer to the type IV isotherm of the mesoporous surface layer of TiO_2.

https://doi.org/10.1346/CCMN.2013.0610301 Published online by Cambridge University Press

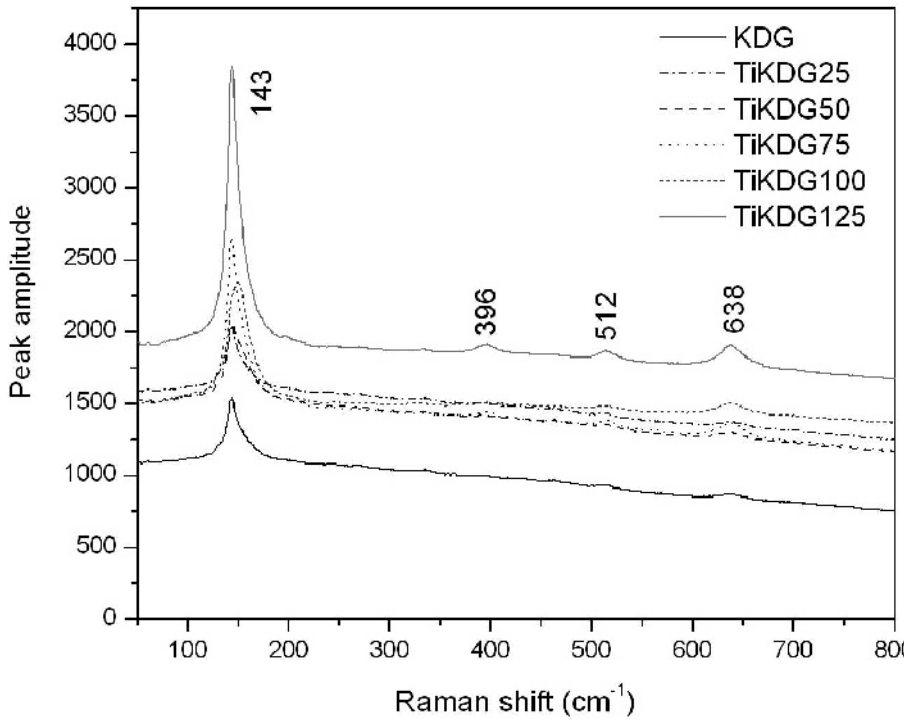

Figure 4. Raman spectra of pure kaolin (KDG) and TiO_2/KDG composites.

With increasing amounts of titania, the surface areas grew linearly, from 46 to 92 m^2g^{-1}. Pure KDG had a surface area of only 12 m^2g^{-1}, but a good covering of the kaolin by a surface layer of TiO_2 particles provided sufficient surface area for adsorption.

The photocatalytic activity of samples prepared in the water phase was determined using the degradation of 0.5 mM RB5 dye aqueous solutions under UV radiation at 365 nm (UV-A, black lamp). As proposed by Zhao *et al.* (2004), the main byproducts formed by the ozonation

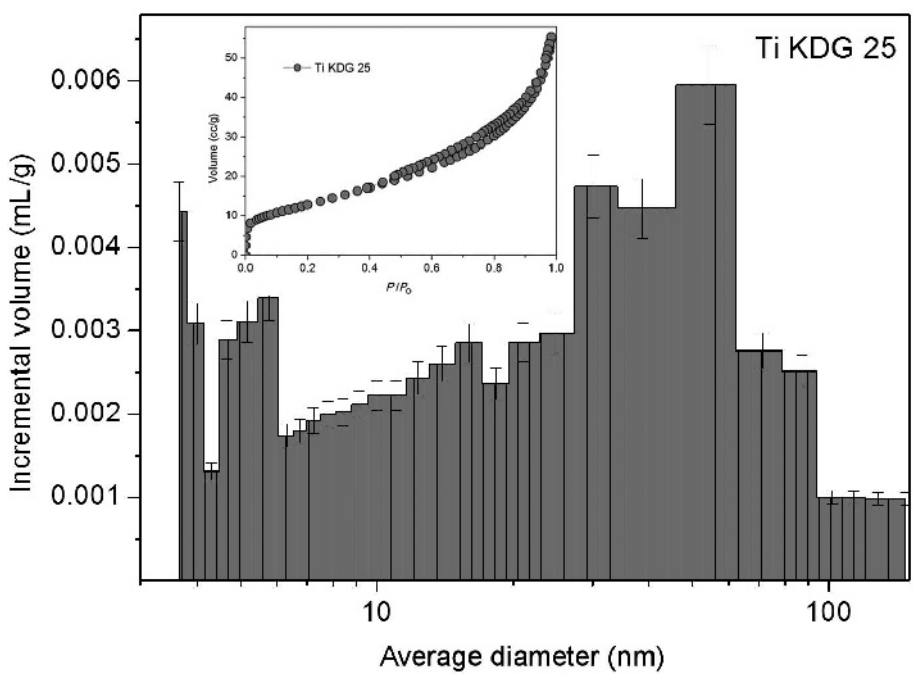

Figure 5. Isotherm (inset) and pore-size distribution of sample TiKDG25.

https://doi.org/10.1346/CCMN.2013.0610301 Published online by Cambridge University Press

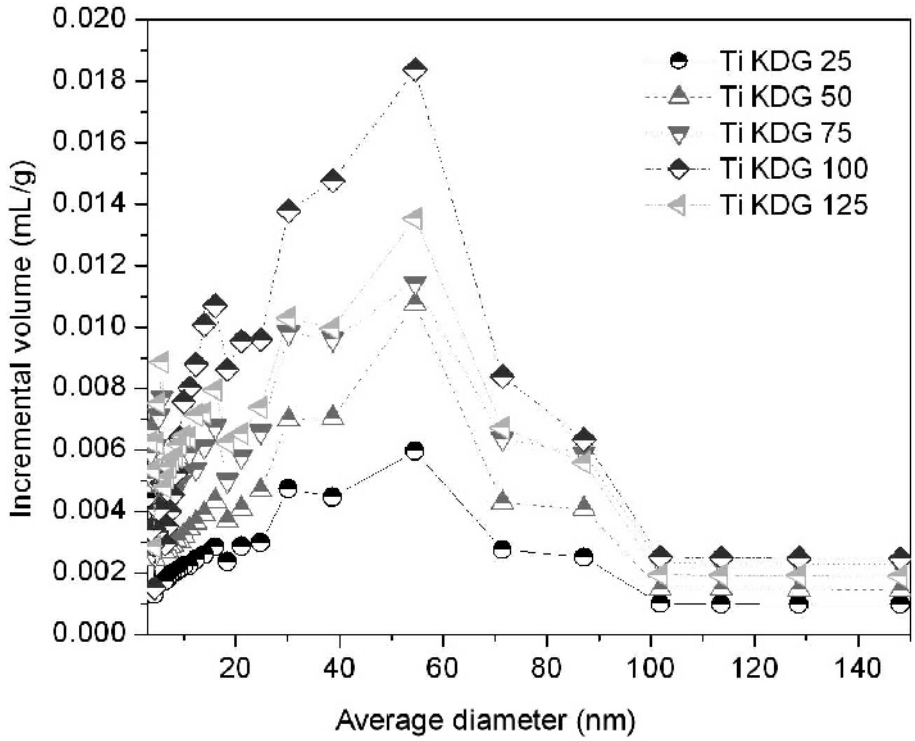

Figure 6. Pore-size distribution of TiO_2/kaolin samples.

or mineralization of azo dyes are organic acids, aldehydes, ketones, and carbon dioxide. According to Demirev and Nenov (2005), the eventual degradation products of azo dyes in the ozonation system are acetic,

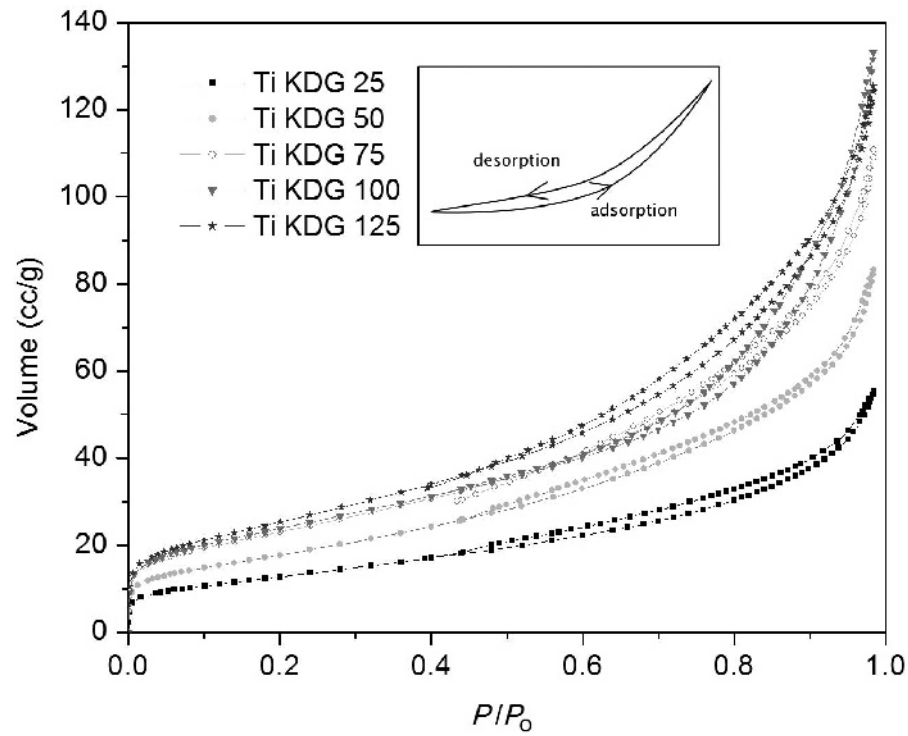

Figure 7. Isotherms of TiO_2/kaolin samples.

https://doi.org/10.1346/CCMN.2013.0610301 Published online by Cambridge University Press

Table 2. Rate constants for RB5 discoloration in water slurries and kinetic parameters for acetone degradation in the gas phase under UV light.

Sample	*k* RB5 (min^{-1})	*k* acetone (h^{-1})	*k* O_2 (h^{-1})	CO	CO_2
Pure TiO_2	0.0257	0.0163	0.0068	1.2	14.9
TiKDG25	0.0430	0.0057	0.0112	5.1	13.2
TiKDG50	0.0247	0.0089	0.0131	4.3	18.2
TiKDG75	0.0323	0.0068	0.0126	0.8	5.4
TiKDG100	0.0299	0.0091	0.0121	2.9	10.2
TiKDG125	0.0391	0.0143	0.0118	2.9	9.7

formic, and oxalic acids. The mechanism of mineralization of RB5 dye in heterogeneous photocatalysis on $SrTiO_3/CeO_2$ was proposed by Song *et al.* (2007). The titania catalyzed the RB5 reaction, and mineralization products were mentioned by Sahel *et al.* (2007) and Damodar and You (2010).

For the assessment of the kinetics of a heterogeneous photocatalytic decomposition of model compounds such as RB5 dye, the Langmuir-Hinshelwood equation (Konstantinou and Albanis, 2004) can be used:

$$r = -d[\text{RB5}]/dt = -\,k_r \cdot K \cdot [\text{RB5}]/(1 + K \cdot [\text{RB5}]) \qquad (5)$$

where r is the degree of dye mineralization, k_r the rate constant, t the illumination time, K the adsorption coefficient of the dye, and [RB5] the dye concentration. When the chemical concentration is a millimolar solution (*i.e.* [RB5]0 is small), equation 4 can be simplified to an apparent first-order equation:

$$\ln \cdot ([\text{RB5}]_0/[\text{RB5}]) = -k_r \cdot K \cdot t \qquad (6)$$

or:

$$[\text{RB5}] = [\text{RB5}]0 \cdot \exp(-k \cdot t); \quad (k = k_r \cdot K) \qquad (7)$$

As can be seen from the calculated rate constants (Table 2) and the kinetic curves under a UV light (Figure 8), the photoactivity of composite samples was surprisingly high, comparable to or even higher than that of pure titania. This is surprising because all of the TiKDG samples had much smaller surface areas than pure titania and a significant proportion of the particles comprised non-active support, so the presumed result would be a rapid decrease of reactivity, which was observed by Rieder *et al.* (2010). However, for the photocatalyzed reaction, the availability of the surface for the incident light is crucial, alongside the adsorption ability of the surface. Even though the kaolin support has much larger particles than pure titania, it can effectively increase titania activity by hindering the agglomeration

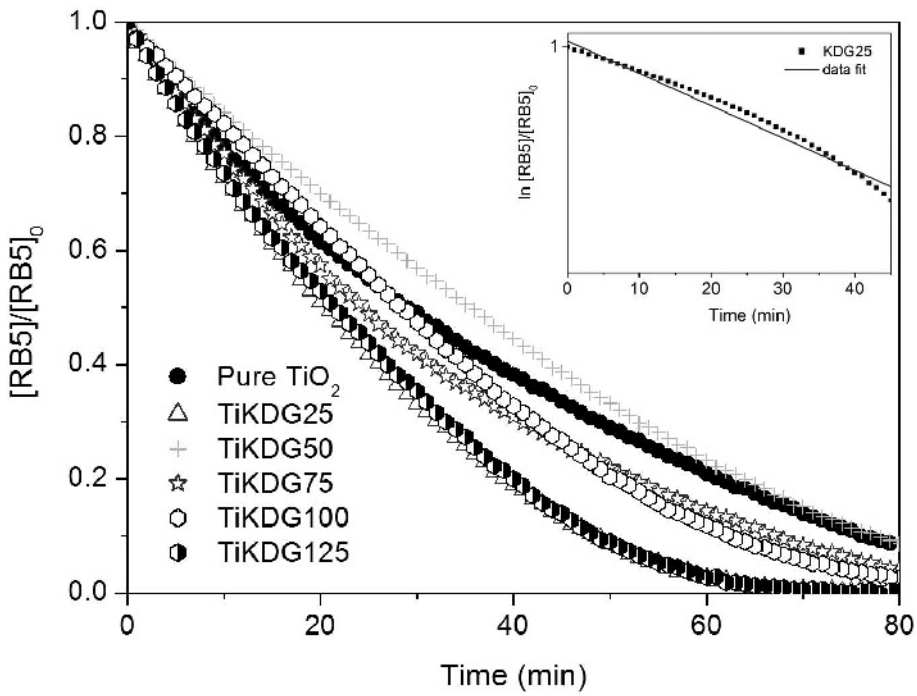

Figure 8. Kinetics of RB5 dye discoloration on TiO_2 and TiO_2/kaolin samples. under UV light.

https://doi.org/10.1346/CCMN.2013.0610301 Published online by Cambridge University Press

of very small titania particles as they become more uniformly distributed on the kaolin surfaces. Moreover, the kaolin particles have only large pores which are readily accessible by the light. Last but not least, the sorption ability of clay minerals in soil is well known and this phenomenon surely contributes to good adsorption of the pollutant (azo dye in this case) on the particle surface, where it can be decomposed.

One of the aims of the present study was to estimate the optimum ratio of the concentration of TiO_2 and supporting kaolin. The rate constants for RB5 decomposition were similar to each other and the largest was observed for sample TiKDG25 with the smallest amount of titania, but note that the second largest was TiKDG125 with the most TiO_2 in the structure. From these results an ideal ratio of substrate and TiO_2 cannot be established, but some valuable information can be gleaned. The rather small amount of titania in sample TiKDG25 was sufficient for effective coverage of the substrate to provide an adequate performance of the active surface layer; larger amounts did not guarantee a further increase in terms of the activity. Good homogeneous distribution on particles of the substrate may be the key property governing performance. The larger dosage of titania led to the formation of more layers on the surface of kaolin, but the diffusion in water suspension is not as rapid and the amount of pollutant adsorbed cannot reach the inner surface and exploit the whole surface of active TiO_2.

Rate constants for acetone degradation, O_2 consumption, and normalized total ion current (TIC) for CO and CO_2 evolution after 45 h (Table 2), and the typical corresponding experimental dependencies in time are presented (Figure 9). The rate of degradation was estimated to obey pseudo-first-order kinetics, and hence the rate constant for degradation, k, was obtained from the first-order plot according to equation 8, where c_0 is the initial concentration, c is the concentration of acetone after time (t), and k is the first-order rate constant:

$$\ln(c/c_0) = -kt \quad (8)$$

Before each measurement the reactor was evacuated and then purged with O_2. When the measured gas chromatogram showed only the oxygen peak, a substance for photocatalytic decomposition (in this case the acetone) could then be injected. The subsequent chromatogram showed the peaks for the O_2 and the acetone, marked with a value of 1. The gases, which were expected to be formed due to a photocatalyzed reaction (CO, CO_2), were assigned zero values. Thus, input data were normalized and measurements over a time period of 2 h could commence.

During the reaction no peaks for intermediates were detected, suggesting that photocatalytic oxidation proceeded not in the gaseous phase but only on the surface layer directly, causing the formation of CO and CO_2.

Sample TiKDG125, which contained the largest amount of titania, had the largest rate constant for acetone degradation; next was sample TiKDG100. However, to evaluate photoactivity, the important parameters are not just the rate but also the degree of mineralization, which is difficult to determine by discoloration of azo dye in water slurries. A gas chromatograph-mass spectroscopy (GC-MS) detection system in a gas-phase identification of the samples

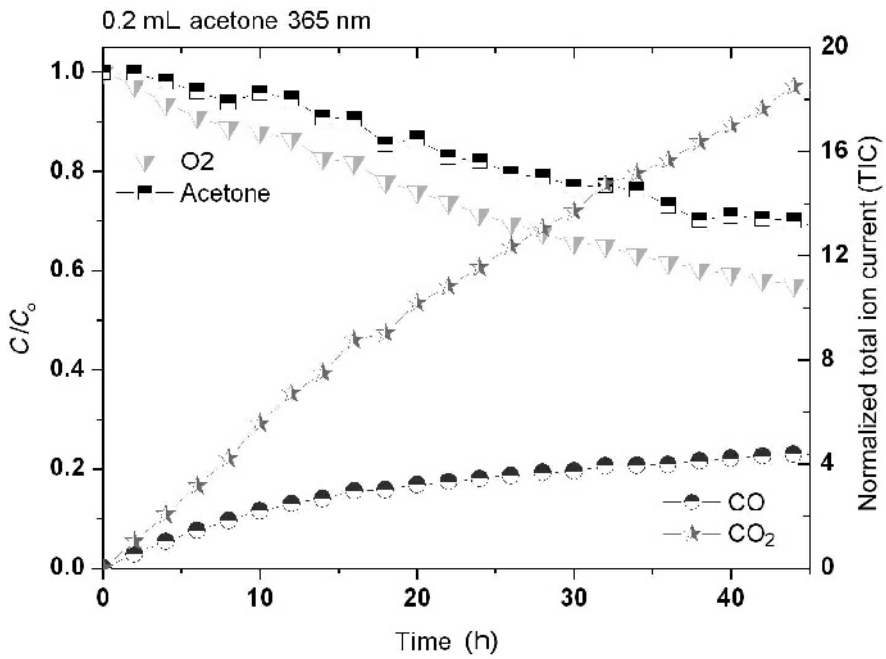

Figure 9. Kinetics of the photocatalytic degradation of acetone on a layer of sample TiKDG50.

https://doi.org/10.1346/CCMN.2013.0610301 Published online by Cambridge University Press

which produced the most CO_2 is possible and might be more relevant. Samples TiKDG50 and TiKDG25 had smaller titania contents and the highest degrees of mineralization, consistent with the data obtained from RB5 discoloration in water slurries, where the titania content and a growing surface area did not lead to greater activity. An obvious conclusion is that both the surface area and the availability of the surface for incident light were crucial parameters. Therefore, a perfectly distributed surface layer of well crystallized particles was desired. What was somewhat surprising was the level of activity of sample TiKDG50 on acetone mineralization in the gas phase, in spite of its lesser activity in RB5 discoloration in water. However, the data for one set of samples for different pollutants in different environments are often not perfectly consistent. The many variable aspects, such as different mechanisms of degradation, adsorption, hydrophobicity, diffusion, *etc*., can affect the photocatalytic activity significantly. As a result, one cannot identify with certainty the perfect photocatalyst for all pollutants in different environments so that variability in the results could be expected. This variability should be the subject of further research.

CONCLUSIONS

The kaolin substrate with a surface layer of TiO_2 was synthesized by the simple 'one-pot' method of homogeneous hydrolysis. Analysis by XRD, IR, and Raman spectroscopy proved that the titania formed was nanocrystalline anatase; no impurities or phase admixtures were found. Titania was deposited on kaolin. The photoactivity of the synthesized composite samples was assessed in water slurries and in the gas phase. The tests proved that a thin surface layer of titania on kaolin was sufficient for good photocatalytic performance in comparison with pure TiO_2. Despite a much smaller surface area of kaolin/TiO_2 compared with pure titania, the activity was surprisingly high, which could be the result of a good covering of plate-like particles of kaolinite with only large pores allowing easy approach of incident light.

Kaolin has much larger particles and could be separated easily from water slurries compared to very small particles of titania. Therefore, the TiO_2 deposited on the substrate kaolinite could be a solution for practical difficulties in the separation of particles after treatment. Furthermore, from an economic point of view, the use of a cheap support material with a functional thin surface layer *via* an environmentally benign method promises 'real' application.

ACKNOWLEDGMENTS

This work was supported by the RVO 61388980 and Ministry of Industry and Trade of the Czech Republic (Project No. FR-TI1/006).

REFERENCES

Ahn, B-T., Kim, E-Y, and Kim, D.S. (2009) Synthesis of mesoporous TiO_2 and its application to photocatalytic activation of methylene blue and *E. coli. The Bulletin of the Korean Chemical Society*, **30**,193–196.

Barrett, E.P., Joyner, L.G., and Halenda, P.P. (1951) The determination of pore volume and area distributions in porous substances. 1. Computations from nitrogen isotherms. *Journal of the American Chemical Society*, **73**, 373–380.

Belessi, V., Lambropoulou, D., Konstantinou, I., Katsoulidis, A., Pomonis, P., Petridis, D., and Albanis, T. (2007) Structure and photocatalytic performance of TiO_2/clay nanocomposites for the degradation of dimethachlor. *Applied Catalysis B–Environmental*, **73**, 292–299.

Bish, D.L. (1993) Rietveld refinement of the kaolinite structure at 1.5 K. *Clays and Clay Minerals*, **41**, 738–744.

Brunauer, S., Emmett, P.H., and Teller, E. (1938) Adsorption of gases in multimolecular layers. *Journal of the American Chemical Society*, **60**, 309–319.

Chang, S.S., Clair, B., Ruelle, J., Beauchêne, J., Di Renzo, F., Quignard, F., Zhao, G.J., Yamamoto, H., and Gril, J. (2009) Mesoporosity as a new parameter for understanding tension stress generation in trees. *Journal of Experimental Botany*, **60**, 3023–3030.

Chen, J.Y., Li, G.Y., He, Z.G., and An, T.C. (2011a) Adsorption and degradation of model volatile organic compounds by a combined titania-montmorillonite-silica photocatalyst. *Journal of Hazardous Materials*, **190**, 416–423.

Chen, K., Li, J., Wang, W., Zhang, Y., Wang, X., and Su, H. (2011b) The preparation of vanadium-doped TiO(2)-montmorillonite nanocomposites and the photodegradation of sulforhodamine B under visible light irradiation. *Applied Surface Science*, **257**, 7276–7285.

Choi, H., Sofranko, A.C., and Dionysiou, D.D. (2006) Nanocrystalline TiO_2 photocatalytic membranes with a hierarchical mesoporous multilayer structure: Synthesis, characterization, and multifunction. *Advanced Functional Materials*, **16**, 1067–1074.

Chong, M.N., Vimonses, V., Lei, S., Jin, B., Chow, C., and Saint, C. (2009) Synthesis and characterisation of novel titania impregnated kaolinite nano-photocatalyst. *Microporous and Mesoporous Materials*, **117**, 233–242.

Choy, J.H., Park, J.H., and Yoon, J.B. (1998) Multilayered SiO_2/TiO_2 nanosol particles in two-dimensional aluminosilicate catalyst-support. *Journal of Physical Chemistry B*, **102**, 5991–5995.

Ctibor, P., Ageorges, H., Stengl, V., Murafa, N., Pis, I., Zahoranova, T., Nehasil, V., and Pala, Z. (2011) Structure and properties of plasma sprayed $BaTiO_3$ coatings: Spray parameters versus structure and photocatalytic activity. *Ceramics International*, **37**, 2561–2567.

Damodar, R.A. and You, S.J. (2010) Performance of an integrated membrane photocatalytic reactor for the removal of Reactive Black 5. *Separation and Purification Technology*, **71**, 44–49.

Demirev, A. and Nenov, V. (2005) Ozonation of two acidic azo dyes with different substituents. *Ozone-Science & Engineering*, **27**, 475–485.

Ding, X.J., An, T., Li, G., Zhang, S., Chen, J., Yuan, J., Zhao, H., Chen, H., Sheng, G., and Fu, J. (2008) Preparation and characterization of hydrophobic TiO_2 pillared clay: The effect of acid hydrolysis catalyst and doped Pt amount on photocatalytic activity. *Journal of Colloid and Interface Science*, **320**, 501–507.

Ding, Z., Zhu, H.Y., Greenfield, P.F., and Lu, G.Q. (2001) Characterization of pore structure and coordination of

titanium in TiO_2 and SiO_2-TiO_2 sol-pillared clays. *Journal of Colloid and Interface Science*, **238**, 267–272.

Farmer, V.C. (1974) *The Infrared Spectra of Minerals*. Monograph **4**, The Mineralogical Society, London.

Guillard, C., Disdier, J., Monnet, C., Dussaud, J., Malato, S., Blanco, J., Maldonado, M.I., and Herrmann, J.-M. (2003) Solar efficiency of a new deposited titania photocatalyst: chlorophenol, pesticide and dye removal applications. *Applied Catalysis B–Environmental*, **46**, 319–332.

Gupta, S.M. and Tripathi, M. (2012) A review on the synthesis of TiO_2 nanoparticles by solution route. *Central European Journal of Chemistry*, **10**, 279–294.

Hamal, D.B. and Klabunde, K.J. (2007) Synthesis, characterization, and visible light activity of new nanoparticle photocatalysts based on silver, carbon, and sulfur-doped TiO_2. *Journal of Colloid and Interface Science*, **311**, 514–522.

Hermosin, M.C., Martin, P., and Cornejo, J. (1993) Adsorption mechanisms of monobutyltin in clay minerals. *Environmental Science & Technology*, **27**, 2606–2611.

ICSD Database (2008) ICSD Database, FIZ Karlsruhe, Germany.

Jiang, Z., Kong, L., Alenazey, F.S., Qian, Y. Xiao, T., and Edwards, P.P. (2013) Enhanced visible-light-driven photocatalytic activity of mesoporous TiO_2-xNx derived from ethylenediamine-based complexes. *Nanoscale*, DOI: 10.1039/C3NR00344B

JCPDS PDF-2 (2001) JCPDS PDF-2. *ICDD*, Newtown Square, PA, USA.

Johnston, C.T., Agnew, S.F., and Bish, D.L. (1990) Polarized single-crystal Fourier-transform infrared microscopy of Ouray dickite and Keokuk kaolinite. *Clays and Clay Minerals*, **38**, 573–583.

Konstantinou, I.K. and Albanis, T.A. (2004) TiO_2-assisted photocatalytic degradation of azo dyes in aqueous solution: kinetic and mechanistic investigations – A review. *Applied Catalysis B–Environmental*, **49**, 1–14.

Kun, R., Mogyorosi, K., and Dekany, I. (2006) Synthesis and structural and photocatalytic properties of TiO_2/montmorillonite nanocomposites. *Applied Clay Science*, **32**, 99–110.

Kutlakova, K.M. Tokarsky, J., Kovar, P., Vojteskova, S., Kovarova, A., Smetana, B., Kukutschova, J., Capkova, P., and Matejka, V. (2011) Preparation and characterization of photoactive composite kaolinite/TiO_2. *Journal of Hazardous Materials*, **188**, 212–220.

Lachheb, H., Puzenat, E., Houas, A., Ksibi, M., Elaloui, E., Guillard, C., and Herrmann, J-M. (2002) Photocatalytic degradation of various types of dyes (Alizarin S, Crocein Orange G, Methyl Red, Congo Red, Methylene Blue) in water by UV-irradiated titania. *Applied Catalysis B–Environmental*, **39**, 75–90.

Li, Q., Xu, Z., Gao, S., and Shang, J.K (2010) As(III) removal by hydrous titanium dioxide prepared from one-step hydrolysis of aqueous $TiCl_4$ solution. *Water Research*, **44**, 5713- 5721.

Mao, H.H., Li, B., Li, X., Yue, L., Xu, J., Ding, B., Gao, X., and Zhou, Z. (2010) Facile synthesis and catalytic properties of titanium containing silica-pillared clay derivatives with ordered mesoporous structure through a novel intra-gallery templating method. *Microporous and Mesoporous Materials*, **130**, 314–321.

Menesi, J., Korosi, L., Bazso, E., Zollmer, V., Richardt, A., and Dekany, I. (2008) Photocatalytic oxidation of organic pollutants on titania-clay composites. *Chemosphere*, **70**, 538–542.

Mogyorosi, K., Farkas, A., Dekany, I., Ilisz, I., and Dombi, A. (2002) TiO_2-based photocatalytic degradation of 2-chlorophenol adsorbed on hydrophobic clay. *Environmental Science & Technology*, **36**, 3618–3624.

Murad, E. (1997) Identification of minor amounts of anatase in kaolins by Raman spectroscopy. *American Mineralogist*, **82**, 203–206.

Ohsaka, T., Izumi, F., and Fujiki, Y. (1978) Raman-spectrum of anatase, TiO_2. *Journal of Raman Spectroscopy*, **7**, 321–324.

Rieder, M., Klementova, M., and Szatmary, L. (2010) High-temperature growth of anatase on kaolinite substrate. *Proceedings of the Royal Society A – Mathematical, Physical and Engineering Sciences*, **466**, 721–730.

Robin, V., Petit, S., Beaufort, D., and Prêt, D. (2013) Mapping kaolinite and dickite in sandstone thin sections using infrared microscopy. *Clays and Clay Minerals*, **61**, 141–151.

Sahel, K., Perol, N., Chermette, H., Bordes, C., Derriche, Z., and Guillard C. (2007) Photocatalytic decolorization of Remazol Black 5 (RB5) and Procion Red MX-5B – Isotherm of adsorption, kinetic of decolorization and mineralization. *Applied Catalysis B – Environmental*, **77**, 100–109.

Saikia, B.J. and Parthasarathy, G. (2010) Fourier Transform infrared spectroscopic characterization of kaolinite from Assam and Meghalaya, northeastern India. *Journal of Modern Physics*, **1**, 206–210.

Sing, K.S.W., Everett, D.H., Haul, R.A.W., Moscou, L., Pierotti, R.A., Rouquerol, J., and Siemieniewska, T. (1985) Reporting physisorption data for gas solid systems with special reference to the determination of surface-area and porosity (Recommendations 1984). *Pure and Applied Chemistry*, **57**, 603–619.

Song, S., Xu, L., He, Z., and Chen, J. (2007) Mechanism of the photocatalytic degradation of CI reactive black 5 at pH 12.0 using $SrTiO_3$/CeO_2 as the catalyst. *Environmental Science & Technology*, **41**, 5846–5853.

Stengl, V., Subrt, J., Bakardjieva, S., Kalendova, A., and Kalenda, P. (2003a) The preparation and characteristics of pigments based on mica coated with metal oxides. *Dyes and Pigments*, **58**, 239–244.

Stengl, V., Subrt, J., Bezdicka, P., Marikova, M., and Bakardjieva, S. (2003b) Homogeneous precipitation with urea – An easy process for making spherical hydrous metal oxides. *Solid State Chemistry V*, **90–91**, 121–126

Stengl, V. and Matys Grygar, T. (2011) The simplest way to iodine-doped anatase for photocatalysts activated by visible light. *International Journal of Photoenergy*, doi:10.1155/2011/685935.

Stengl, V., Houskova, V., Bakardjieva, S., Murafa, N., and Havlin, V. (2008a) Optically Transparent Titanium Dioxide Particles Incorporated in Poly(hydroxyethyl methacrylate) Thin Layers. *Journal of Physical Chemistry C*, **112**, 19979–19985.

Stengl, V., Bakardjieva, S., Murafa, N., and Houskova, V. (2008b) Hydrothermal synthesis of titania powders and their photocatalytic properties. *Ceramics-Silikaty*, **52**, 278–290.

Stengl, V., Bakardjieva, S. and Murafa, N. (2009) Preparation and photocatalytic activity of rare earth doped TiO_2 nanoparticles. *Materials Chemistry and Physics*, **114**, 217–226.

Trentler, T.J., Denler, T.E., Bertone, J.F., Agrawal, A., and Colvin, V.L. (1999) Synthesis of TiO_2 nanocrystals by nonhydrolytic solution-based reactions. *Journal of the American Chemical Society*, **121**, 1613–1614.

Vimonses, V., Chong, M.N., and Jin, B. (2010) Evaluation of the physical properties and photodegradation ability of titania nanocrystalline impregnated onto modified kaolin. *Microporous and Mesoporous Materials*, **132**, 201–209.

Wang, C.C. and Ying, J.Y. (1999) Sol-gel synthesis and hydrothermal processing of anatase and rutile titania nanocrystals. *Chemistry of Materials*, **11**, 3113–3120.

Yamanaka, S., Nishihara, T., Hattori, M., and Suzuki, Y. (1987) Preparation and properties of titania pillared clay. *Materials Chemistry and Physics*, **17**, 87–101.

Yang, X., Zhu, H., Liu, J., Gao, X., Martens, W.N., Frost, R.L., and Shen, Y., Yuan, Z. (2008) A mesoporous structure for efficient photocatalysts: Anatase nanocrystals attached to leached clay layers. *Microporous and Mesoporous Materials*, **112**, 32–44.

Zhao, W.R., Shi, H.X., and Wang, D.H. (2004) Ozonation of cationic Red X-GRL in aqueous solution: degradation and mechanism. *Chemosphere*, **57**, 1189–1199.

(*Received 2 July 2012; revised 22 March 2013; Ms. 686; AE: P.B. Malla*)